Mon. Not R. astr. Soc. (1982) **201**, 745–758

The interrelation of cosmic γ-rays and interstellar gas in the range l:65–180°

K. Arnaud, Li Ti pei*, P. A. Riley and A. W. Wolfendale
Department of Physics, University of Durham, South Road, Durham DH1 3LE
T. M. Dame, J. E. Brock and P. Thaddeus *Goddard Institute for Space Studies, New York, USA*

Received 1982 March 29; in original form 1981 October 26

Summary. New data on the distribution of molecular hydrogen in the first and second quadrants allow a detailed analysis of the relationship between the column density of gas (in all major forms) and the intensity of cosmic γ-rays in the Galaxy.

It is concluded that most of the features observed in the gamma-ray map can be explained in terms of cosmic-ray interactions with the gas in the ISM, with molecular hydrogen playing an important rôle. The cosmic-ray intensity in the important production regions appears to be roughly independent of galactocentric distance, R, for l:65–100° and to fall off slowly with R for l:100–180°.

1 Introduction

The γ-ray 'sky' is composed of an uncertain mixture of contributions from discrete sources (pulsars, etc.) and from a 'continuum' arising from cosmic-ray interactions with the gas in the ISM. Both contributions are of importance, the former because of the relationship of γ-rays to the other energetic processes occurring in the immediate environment of the exotic objects and the latter because of the possibility that by studying the spatial distribution of the initiating cosmic rays, information might accrue on the outstanding problem of the origin of cosmic rays.

Insofar as gas in the Galaxy is clumped, this feature being particularly marked for molecular hydrogen, there is the possibility of distant gas clouds, irradiated by the ambient cosmic-ray flux, being mistaken for discrete sources. Thus, a detailed analysis of the ISM is important, both to distinguish genuine discrete sources from irradiated clouds and to examine the spatial distribution of cosmic rays. A number of studies of this type have been made but a serious drawback has been the lack of availability of data on H_2 for much of the Galaxy. Thus, much earlier work has concentrated on 'high' latitudes, e.g. $|b| > 10°$ (Lebrun

* On leave from the Institute of High Energy Physics, Academy of Sciences, Beijing, China.

& Paul 1979; Strong & Wolfendale 1981) where galaxy counts have been used to make rough estimates of the total gas content and on regions of the Galaxy where atomic hydrogen predominates (e.g. Issa *et al.* 1981a).

Very recently, H_2 column densities (inferred from CO line measurements) have started to become available for significant regions of space in and near the galactic plane in the longitude range considered here and this has allowed the rôle of molecular hydrogen in gamma-ray astronomy to be examined. The first extensive range was that covered by Cohen *et al.* (1980); l: 105–139°, $|b| < 3°$ and in a recent paper (Li & Wolfendale 1981a) we made a detailed examination of that region. The Columbia instrument has since yielded more CO data and in the present work we examine in some detail another region, l: 65–180°, b: $-5°$ to $+6°$ or $+10°$ (the limit varying somewhat with l). If, as we have claimed previously, there is a large-scale gradient of cosmic-ray intensity in the Galaxy with a slow fall-off of intensity with galactocentric radius, R, for $R \lesssim 5$ kpc, then, for part of the range, l: 65–100° (to be denoted by 'Range I') much of the emission detected at the Earth will have come from regions with $R \simeq 10$ kpc, i.e. where the cosmic-ray intensity is close to that observed locally. In consequence we would expect the observed flux here to be well represented by the product of the column density of total gas and the local γ-ray emissivity ($q/4\pi = 2.2 \times 10^{-26}$ (H atom)$^{-1}$ s^{-1} sr^{-1} for $E_\gamma > 100$ MeV; Issa *et al.* 1981a; Issa, Riley & Wolfendale 1981b) assuming that genuine discrete sources are not contributing appreciably. A further point of importance is that the derivation of H_2 column densities should not be affected by the rather uncertain 'metallicity gradient' in the Galaxy because here R is approximately constant.

In the other part of the longitude range, l: 100–180° (to be denoted by 'Range II') the situation is different in that the likely fall-off of cosmic-ray intensity with R is important and amenable to study.

In what follows, we describe the source of data on gas densities and on γ-ray fluxes and go on to make a detailed comparison of our predicted fluxes with those observed, the principal objective being to examine the rôle of H_2 clouds as either targets for the ambient cosmic-ray flux (or for an enhanced flux) or as the sites of γ-ray sources.

2 Column densities of gas

2.1 ATOMIC HYDROGEN

The standard Berkeley measurements of Weaver & Williams (1973) are used to give $\int T dv$ and finite optical depth is allowed for by adopting a mean gas temperature of 120 K, following Burton (1976). The magnitude of the correction for optical depth is, typically, a factor 1.20 at $l = 90°$, $b = 0°$. Recent work by us, to be published later, suggests that the column densities may be still underestimated by as much as 20 per cent as one approaches $l \simeq 180°$; this point is taken up again later. The column densities have been converted to trial γ-ray intensities under the assumption that the cosmic-ray intensity is the same everywhere and that the γ-ray emissivity is as given in Section 1. A correction has been applied to allow for the point spread function of the *COS-B* instrument; following Hermsen 1980, we use the function $f(\theta) = k \exp -(\theta/\theta_0)^{2c}$ where θ is the angle between the apparent and real γ-ray arrival directions and θ_0 and c are constants; for the energy of major concern here, $E_\gamma > 100$ MeV, $\theta_0 = 1.25°$ and c = 0.5.

Figs 1(a) and 2(a) show the contours of predicted γ-ray intensity for H I as target.

2.2 MOLECULAR HYDROGEN

The CO data are those of Thaddeus and co-workers: the Columbia group (Cohen *et al.* 1980; Dame & Thaddeus, to be published; see also Thaddeus 1981). In this work, $\int T(^{12}\mathrm{CO})\,dv$ is

given as a function of l and b (T being the antenna temperature) and we have converted to column densities of H_2 using for the conversion the expression: $N(H_2) = 2.3 \times 10^{20} \int T(^{12}CO)\, dv$ molecules cm^{-2} (following Gordon & Burton 1976). It is realized that the conversion factor is the source of debate; a discussion is given later.

Figs 1(b), 2(b) and (c) show the trial γ-ray intensities, again convolved with the *COS-B* point spread function (PSE) for γ-ray energies above 100 MeV. In Fig. 2 division has been made into 'near' and 'far', where 'near' comprises material selected by velocity information at galactocentric distance, $R < 12$ kpc and 'far' relates to $R > 12$ kpc, adopting the rotation curve of Burton & Gordon (1978). The boundary of R is, of course, sensitive to the rotation curve used; adopting instead a flat rotation curve beyond $R = 10$ kpc (probably the upper limit), with $V = 250$ km s^{-1}, the boundary changes from 12 kpc to 12.6 kpc – such a change does not alter our conclusion significantly. (The possibility of the conversion $CO \rightarrow N(H_2)$ depending on radial distance is taken up later.) It is interesting to note the similarities and the differences between the distributions of H I and H_2.

2.3 OTHER ELEMENTS IN THE ISM

It is assumed implicitly that the standard ISM composition is appropriate to all regions, in particular that the total number of nucleons is 1.4 times the number of H-nuclei (the nuclei being in H I or H_2), Dodds, Wolfendale & Wdowczyk (1976) and the elements with $Z > 1$ are allowed for in the γ-ray emissivity factor adopted. The metallicity variations which undoubtedly occur are unlikely to cause an error of more than about 10 per cent in the total column density from this cause. The effect of metallicity gradients on the $CO \rightarrow N(H_2)$ conversion is much more serious.

Ionized gas is also a problem but with a likely density of only 3×10^{-2} cm^{-3} (from pulsar observations) its contribution is probably only about 20 per cent at $b = 5°$, compared with atomic hydrogen, and somewhat smaller at lower latitudes.

3 Gamma-ray data

3.1 INTENSITY CONTOURS

The γ-ray data used in the present work are from the *SAS-2* and *COS-B* experiments, with more emphasis being placed on the latter. The *COS-B* results used are those presented in papers by Mayer-Hasselwander *et al.* (1980, 1982) which relate to the energy ranges 70–150, 150–300 and 300–5000 MeV.

We also use the detailed analysis of γ-ray 'sources' given by Hermsen (1980, 1981). Figs 1(d) and (e) and 2(e) and (f) give illustrative contours from the work of Mayer-Hasselwander *et al.* (1982).

The *SAS-2* results used are those published in tabular form by Fichtel *et al.* (1978). We have generated contour maps for $E_\gamma > 100$ MeV from the data and these are given in Figs 1(f) and 2(g). The total numbers of γ-rays detected by the *SAS-2* telescope in the latitude range indicated and in longitude bins 3° wide, are shown above the maps. Because of the small number of events recorded by *SAS-2*, a large bin size, $3 \times 3°$, was employed when making the maps so that the resolution is degraded a little.

The numbers of γ-rays represented by the *COS-B* contours are an order of magnitude larger than in the *SAS-2* case but the increased (non-cosmic) background means that the contours are not 'superior' by this same factor.

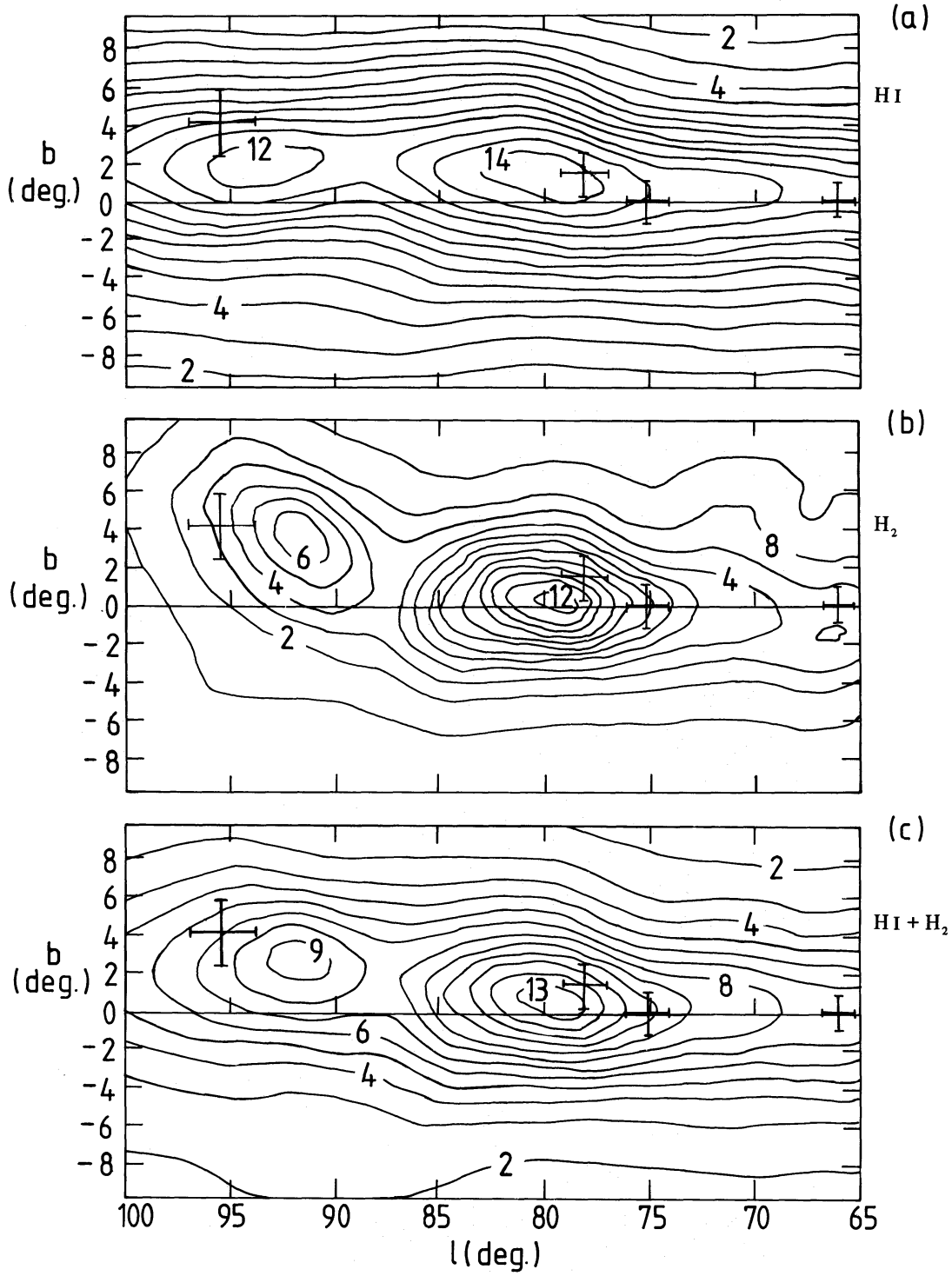

Figure 1. (a) Contours of γ-ray intensity ($E_\gamma > 100$ MeV) expected for constant cosmic-ray intensity with atomic hydrogen alone as target material. A smoothing with the *COS-B* point spread function for $E\gamma > 100$ MeV has been applied. Intensity levels: $I_\gamma = (2n - 1.5)\ 10^{-5}\ \mathrm{cm^{-2}\,s^{-1}\,sr^{-1}}$. The *COS-B* 'sources' from the 2CG catalogue of Hermsen (1981) are indicated. (b) As (a) but for molecular hydrogen alone. Intensity levels: $I_\gamma = (2n - 5)\ 10^{-5}\ \mathrm{cm^{-2}\,s^{-1}\,sr^{-1}}$. (c) As (a) but for H I and H_2 together. Intensity levels: $I_\gamma = (4n - 3)\ 10^{-5}\ \mathrm{cm^{-2}\,s^{-1}\,sr^{-1}}$. (d) *COS-B* γ-ray intensities for E_γ: 150–300 MeV from the data of Mayer-Hasselwander *et al.* (1982). Intensity levels: multiples of $3 \times 10^5\ \mathrm{cm^{-2}\,s^{-1}\,sr^{-1}}$. (e) As (d) but for 300–5000 MeV. Intensity levels: multiples of $4 \times 10^{-5}\ \mathrm{cm^{-2}\,s^{-1}\,sr^{-1}}$. (f) *SAS-2* γ-ray intensity contours for $E_\gamma > 100$ MeV derived by us from the tabulated data of Fichtel *et al.* (1978). The intensities are in units of $10^{-5}\ \mathrm{cm^{-2}\,s^{-1}\,sr^{-1}}$. The symbols mark the positions of the claimed *COS-B* sources (Hermsen 1981). The number of γ-rays contributing per 3° bin of longitude is indicated along the top of the graph.

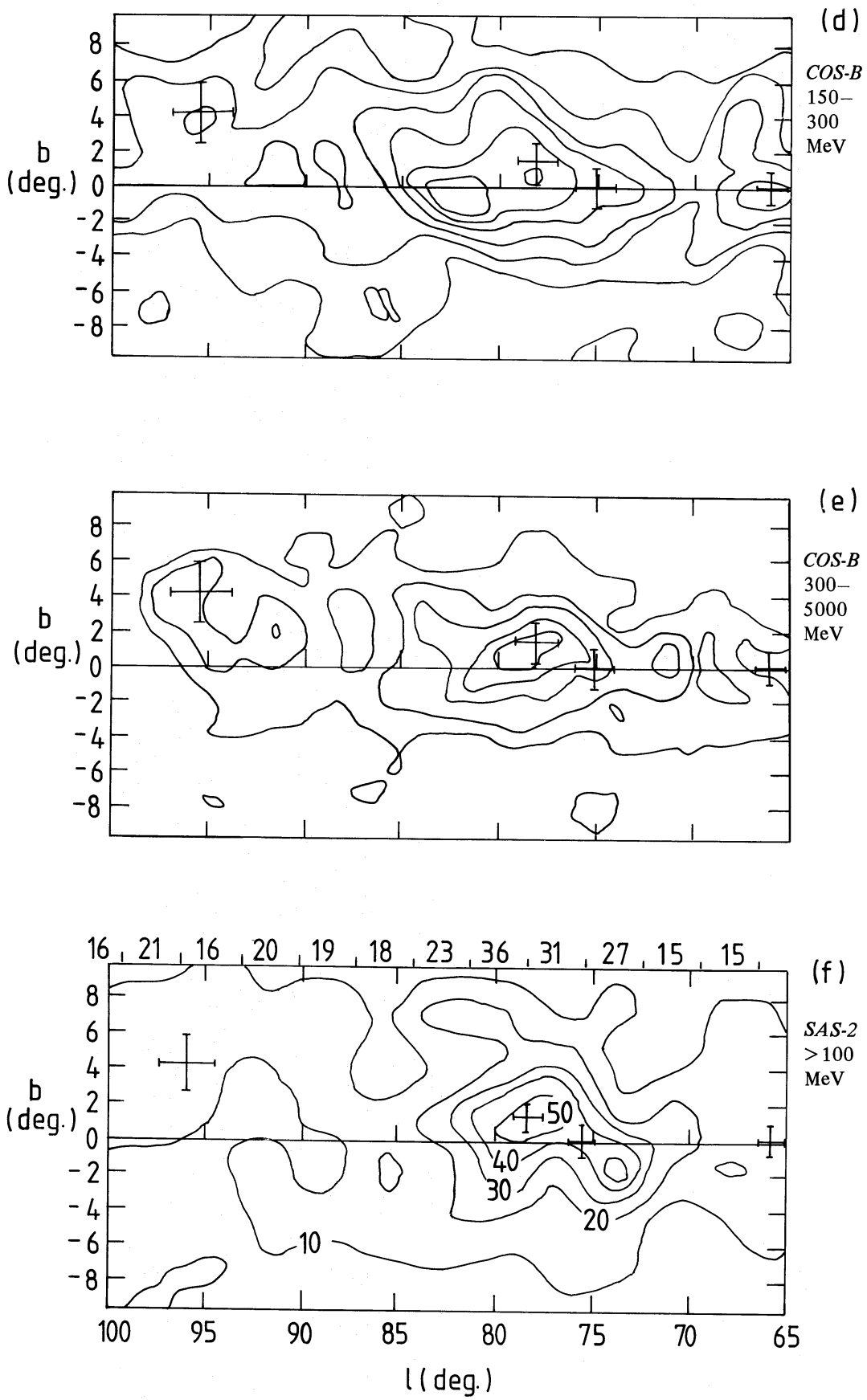

Figure 1 – *continued*

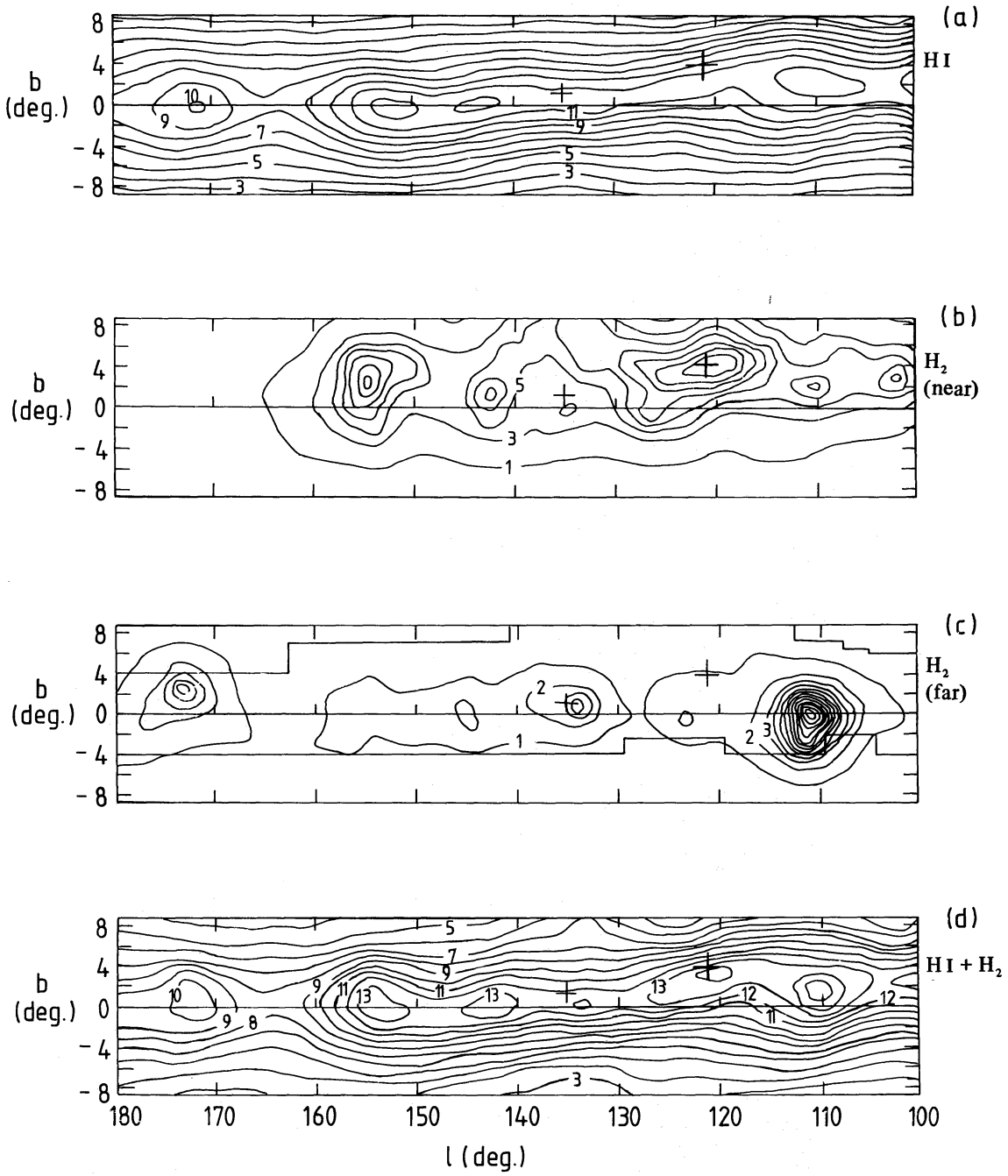

Figure 2. (a) Contours of γ-ray intensity ($E_\gamma > 100$ MeV) expected for constant cosmic-ray intensity with atomic hydrogen alone as target material. A smoothing with the *COS-B* point spread function for $E_\gamma > 100$ MeV has been applied. Intensity levels: $I_\gamma = n\ 1.5 \times 10^{-5}$ cm^{-2} s^{-1} sr^{-1}. The *COS-B* 'sources' from the 2CG catalogue of Hermsen (1981) are indicated. (b) As (a) but for interactions with 'near' molecular hydrogen ($R \lesssim 12$ kpc for adopted rotation curve). Intensity levels: $I_\gamma = (3n - 2)\ 10^{-6}$ cm^{-2} s^{-1} sr^{-1}. (c) As (a) but for 'far' molecular hydrogen ($R \gtrsim 12$ kpc). Intensity levels: I_γ $(3n - 2)\ 10^{-6}$ cm^{-2} s^{-1} sr^{-1}. (d) As (a) but for H I and H_2 together. Intensity levels: $I_\gamma = n\ 1.5 \times 10^{-5}$ cm^{-2} s^{-1} sr^{-1}. (e) *COS-B* γ-ray intensities for E_γ: 150–300 MeV from the data of Mayer-Hasselwander *et al.* (1982). Intensity levels: units of 3×10^{-5} cm^{-2} s^{-1} sr^{-1}. (f) As (e) but for 300–5000 MeV. Intensity levels: units of 4×10^{-5} cm^{-2} s^{-1} sr^{-1}. (g) *SAS-2* γ-ray intensities for $E_\gamma > 100$ MeV derived by us from the tabulated data of Fichtel *et al.* (1978). The intensities are in units of 10^{-5} cm^{-2} s^{-1} sr^{-1}. The symbols mark the positions of the claimed *COS-B* sources (Hermsen 1981). The number of γ-rays contributing per 3° bin of longitude is indicated along the top of the graph. In the blank area, the statistical accuracy is so low that the contours would not be meaningful.

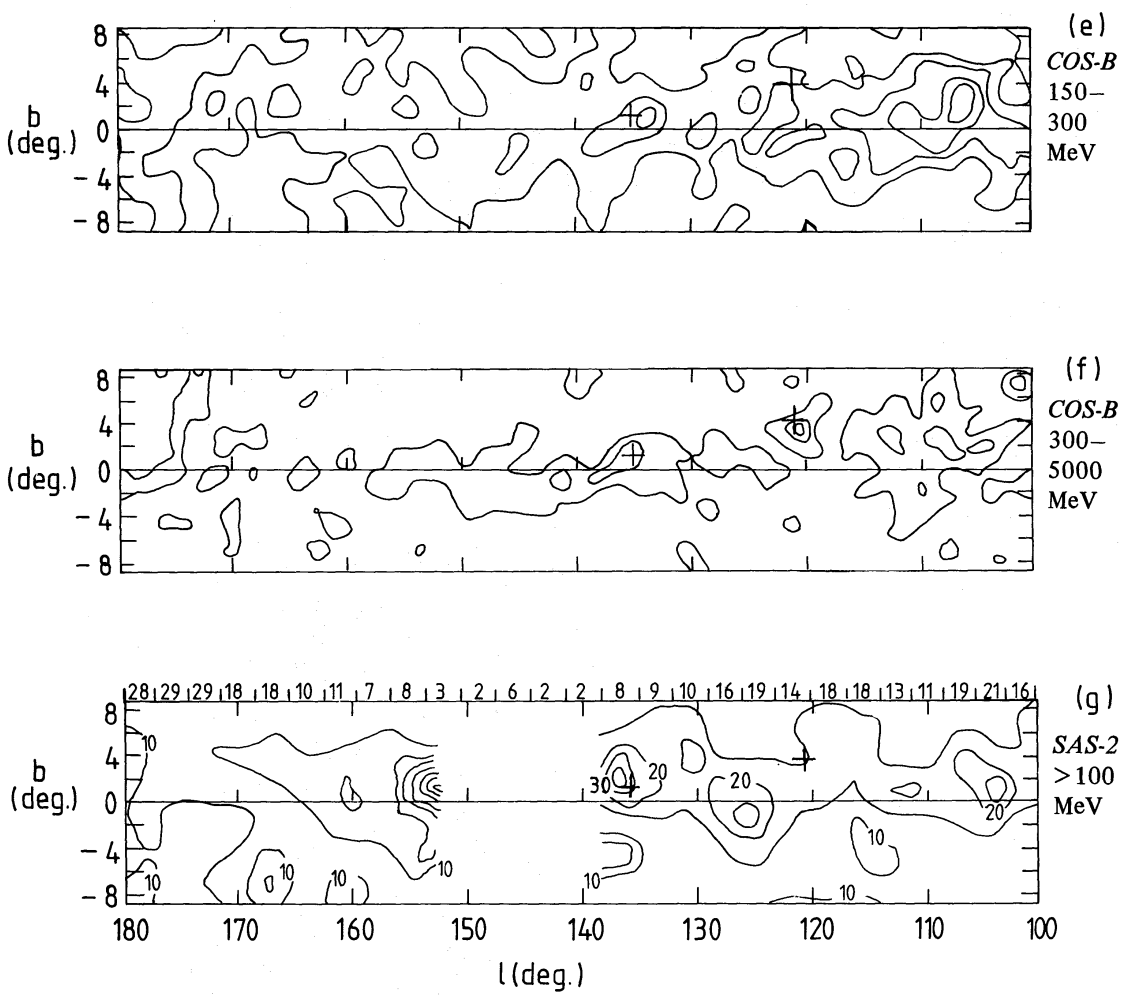

Figure 2 – *continued*

3.2 GAMMA–RAY 'SOURCES'

It is useful at this stage to consider the situation with regard to γ-ray 'sources'. The positions of the 'sources' from the *COS-B* 2CG catalogue of Hermsen are indicated in the figures. A 2CG source is defined as a significant excess above the local background flux which has a spatial distribution consistent with the point spread function of the telescope. A cross-correlation technique was used by the *COS-B* workers to select such sources and to be acceptable it was demanded that the significance of the sources should be better than 4.8 σ. This requirement, together with the limitation imposed by the low numbers of γ-rays detected by *COS-B*, resulted in a lower limit to the detectable flux for such a source near to the galactic plane of about 1.0×10^{-6} photons $cm^{-2} s^{-1}$ ($E_\gamma > 100$ MeV).

The upper limit to the source diameter which would remain unresolved by the *COS-B* telescope is a matter of debate; Hermsen quotes 1–2 degrees for objects in the 2CG catalogue, whereas Li & Wolfendale (1981b) show that some of these sources may have diameters as large as 4°. The relevance of these remarks is that the latter authors claim that a sizeable fraction of the sources are giant molecular clouds irradiated by the ambient cosmic-ray flux and should thus have finite extent. (Some of the disagreement may come from the question of definition of 'size'; Li & Wolfendale consider uniformly emitting circular discs whereas the *COS-B* workers' figure is probably nearer to the FWHM.) Irrespective of the question of

source 'size', however, there is argument about the extent to which the lumpy gas distribution irradiated by CR can give rise to apparent sources. This problem is particularly severe when the number of γ-rays detected is rather low (only $\simeq$ 50–90 per 'source' in many cases for $E_\gamma > 100$ MeV and fluxes $\simeq 1.0 \times 10^{-6}$ cm^{-2} s^{-1}). Insofar as the observed sources only contribute a small fraction to the total flux (and a separate paper will give a detailed examination of their significance) the present work will refer only briefly to them.

4 Comparison of predicted and observed γ-ray results

4.1 RANGE I (l:65–1000°)

4.1.1 Intensity contours

Fig. 1(c) gives the predicted contours for $E_\gamma > 100$ MeV and is directly comparable with Fig. 1(f) which relates to the *SAS-2* experiment. It is immediately seen that there is rough agreement in shape of the contours in the range l:70–85° and in fact the average γ-ray intensities are similar. The peak predicted intensity (at $l \sim 79°$, $b \sim +1°$, Fig. 1c) is $\sim 5.0 \times 10^{-4}$ cm^{-2} s^{-1} sr^{-1} and the observed peak is $\sim 5.5 \times 10^{-4}$ from Fig. 1(f).

Accurate contours for I_γ (> 100 MeV) have not been given for the *COS-B* experiment but we have used the contours for the energy ranges 150–300 MeV and 300–5000 MeV (Fig. 1d and 1e) and contours for the lowest energy range 75–150 MeV (not shown), also given by Mayer-Hasselwander *et al.* (1982), to derive the intensity versus longitude at $b = 0°$. Fig. 3 shows this distribution where the cut along $b = 0°$ for the contours of Fig. 1(c) is also shown. In the region $l \sim 80°$ there is, as for *SAS-2*, good agreement between observation and expectation. Previously (Protheroe, Strong & Wolfendale 1979), basing our arguments on earlier data, we suggested a somewhat higher average cosmic-ray intensity in the general direction of the Cygnus region and more recently (Issa & Wolfendale 1981) we treated 2CG 075+00 and 2CG 078+01 as representing a large molecular cloud complex in the Cygnus arm irradiated by a cosmic-ray intensity higher than locally by a factor 2–5. It is

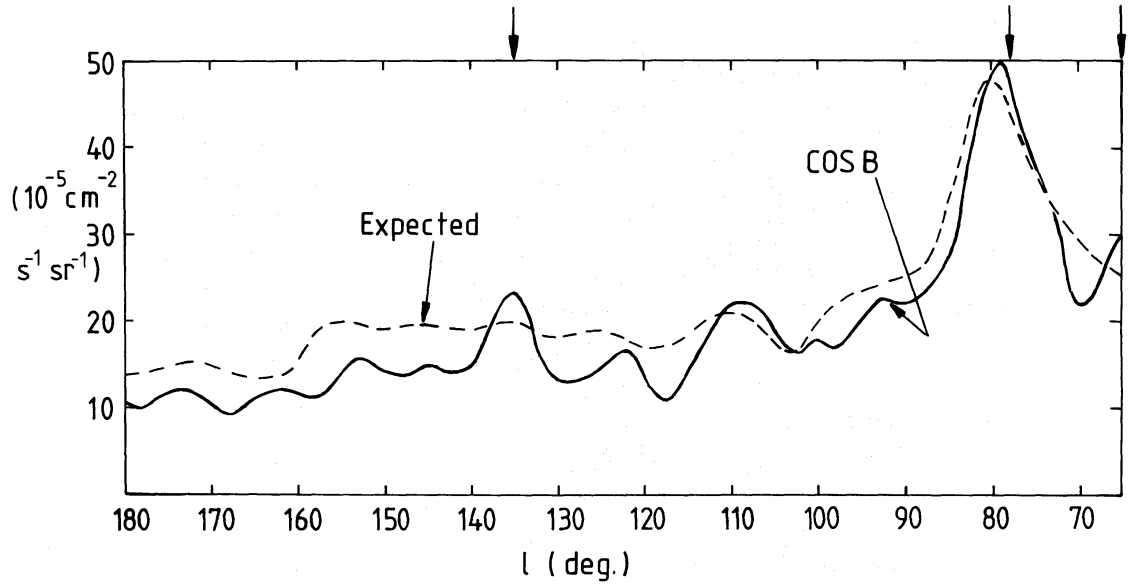

Figure 3. Dependence of γ-ray intensity ($E_\gamma > 100$ MeV) on longitude along $b = 0°$ for the *COS-B* experiment taken from the contours of Mayer-Hasselwander *et al.* (1982). The prediction is for the case where the cosmic-ray intensity everywhere is the same as that locally and the q-value is equal for H I and H_2 and is the same as that needed to explain the γ-ray intensity at 'high' latitudes ($|b| > 10°$) found in other work.

apparent that the increase for this cloud complex (which straddles $b = 0°$) and which contributes about half the column density of gas (see Fig. 1a and b) may not need to be so large, although, as will be shown later (Section 4.1.4) relaxing the condition that the emissivity for H I and H_2 should be the same leads to a higher value for H_2 ($q/4\pi = 3.35 \times 10^{-26}$ cm^{-2} s^{-1} sr^{-1} above 100 MeV compared with the expected 2.2×10^{-26}) which could correspond to a somewhat higher cosmic-ray intensity.

Moving to the range l: 85–100°, comparison of our prediction with the *COS-B* data looks hopeful in that Fig. 1(c) – the prediction – and Fig. 1(d) and (e) all indicate a peak near $l \sim 91°$, $b \sim +2°$. The predicted intensity is $\simeq 2.5 \times 10^{-4}$ cm^{-2} s^{-1} sr^{-1} to be compared with a *COS-B* value of $\simeq 2.5 \times 10^{-4}$. Comparison with *SAS-2* is less reassuring; Fig. 1(f) indicates an intensity at $l \sim 91°$, $b \sim +2°$ of only 1.0×10^{-4} cm^{-2} s^{-1} sr^{-1}, although the uncertainty is large because of the poor statistics.

The situation in the range 65–75° is not very promising. Although there is rough agreement between *SAS-2*, *COS-B* and our predictions in the middle of the range (specifically, at $l \sim 70°$, $b \sim 0°$: 2.0, 2.2 and 2.9×10^{-4} cm^{-2} s^{-1} sr^{-1}) the enhanced region found by *COS-B* near $l = 66°$, $b = 0°$ is not reproduced in *SAS-2* or in our predictions.

4.1.2 *Significance of H_2 as a target for cosmic rays*

It is apparent from the preceding that there is modest agreement between observation and prediction when both H I and H_2 are included as target material. Insofar as the main thrust of the present work is the demonstration of the importance of H_2 it is incumbent on us to demonstrate the improvement in fit between observation and prediction when H_2 is included. This can be done by examining the goodness of fit for the situations H I alone and H I + H_2 together.

Table 1(a) shows the results for the application of the standard relations (Issa *et al.* 1981a and other workers) of the general form:

$$I_\gamma = \frac{q(\mathrm{H\,I})}{4\pi} N(\mathrm{H\,I}) + \frac{q(\mathrm{H_2})}{4\pi} N(\mathrm{H_2})$$

where I_γ is the γ-ray intensity, N(H I) is the column density of H I and $N(H_2)$ is the column density of H_2 (in protons cm^{-2}). In the relation q(H I) and $q(H_2)$ are the appropriate emissivities. In this analysis we have used the data presented by Mayer-Hasselwander *et al.* (1982) for energies E_γ: (150–300) MeV ($|b| < 5°$) and E_γ: (300–5000) MeV ($|b| < 4°$). It might be thought that information is being lost by not binning into latitude as well as longitude bins but in fact much of the latitude dependence within 4 or 5° is instrumental. For the comparison just referred to we have derived the emissivity q(H I) for the condition $q(H_2) = 0$, i.e. disregarding H_2; this is denoted q_{10} and $q(\mathrm{H\,I}) = q(H_2)$ for the situation where our N(H) values are assumed to be quite accurate and the q-values are thus the same for H I and H_2, denoted q_{12}.

Inspection of Table 1(a) shows that the value of χ^2 falls considerably when H_2 is included and that the case where H_2 is disregarded is unacceptable. It should be noted, however, that even when H_2 is included the fit is not very good, particularly in the highest energy region (this point is taken up again later).

4.1.3 *Discrete 'sources'*

The discussion here can be brief. The dominant 'source' 2CG 078 + 01 is clearly associated with the peak in the H_2 complex and although it *could* be a discrete source it is not unlikely

Table 1. (a) Gamma-ray emissivities for the range l: 65–100°: effect of inclusion of H_2 ($q/4\pi$ in units of 10^{-26} cm^{-2} s^{-1} sr^{-1}).

E_γ	$q_{10}/4\pi$	χ^2	$q_{12}/4\pi$	χ^2
150–300 MeV	0.97 ± 0.03	90.6	0.74 ± 0.03	63.1
300–5000 MeV	0.74 ± 0.03	91.5	0.56 ± 0.02	57.4
>70 MeV	3.65 ± 0.06	95.5	2.73 ± 0.05	33.2

Notes
q_{10} relates to the situation where the presence of H_2 is disregarded; for q_{12} it is assumed that the q values of H I and H_2 are the same and H_2 is included. Number of degrees of freedom: 35.

Table 1. (b) Gamma-ray emissivities for the range l: 65–85°: relative effects of H I and H_2.

E_γ	$q_{12}/4\pi$ $\times 10^{-26}$ cm^{-2} s^{-1} sr^{-1}	χ^2	$q_1/4\pi$ $\times 10^{-26}$ cm^{-2} s^{-1} sr^{-1}	$q_2/4\pi$ $\times 10^{-26}$ cm^{-2} s^{-1} sr^{-1}	q_1, q_2 χ^2
150–300 MeV	0.77 ± 0.03	26.6	0.54 ± 0.14	1.34 ± 0.33	23.7
300–5000 MeV	0.54 ± 0.02	42.5	0.21 ± 0.12	1.3 ± 0.2	30.3
>100 MeV	1.70 ± 0.04		1.0 ± 0.2	3.35 ± 0.5	

Notes
q_{12} relates to the situation where the q-values of H I and H_2 are required to be equal; for q_1 and q_2 they are not. Number of degrees of freedom: 20.

that it forms, with 2CG 075 + 00, 'an extended feature'. Hermsen (1981) also considers this to be a possibility. There are also claims for a variable source in this vicinity (at $l \sim 80°$, $b \sim -1°$; Hermsen 1980; Bloemen *et al.* 1981); the present analysis can say nothing about this.

The source 2CG 065 + 00 is not expected from the cosmic-ray interaction process and is presumably genuine but 2CG 095 + 04, the remaining 'source' in Range I seems rather suspect in the sense that *SAS-2* saw nothing despite a modest number of detected γ-rays in that region.

4.1.4 Derivation of γ-ray emissivities

The procedure of Section 4.1.2 has been repeated relaxing the condition that the q-values for H I and H_2 should be the same, this allows for the possibility of conversion errors in deriving the H_2 densities, intensity enhancements in molecular clouds, etc. The analysis here is restricted to the range l: 65–85° to increase still further the likelihood of the cosmic-ray intensity being nearly constant over the production regions. The results are shown in Table 2 for the energy ranges studied (150–300 MeV and 300–5000 MeV); also shown are the approximate values for $E_\gamma > 100$ MeV derived from the sum of the q-values for the two energy ranges and multiplying by an average spectral-shape factor.

Table 2. Gamma-ray emissivities for the range 100–180° ($q/4\pi$ in units of 10^{-26} cm^{-2} s^{-1} sr^{-1}) H_2 neglected.

E_γ	l: 100–140°	l: 140–180°
150–300 MeV	0.88 ± 0.13	0.47 ± 0.08
300–5000 MeV	0.48 ± 0.1	0.37 ± 0.07
>100 MeV	1.7 ± 0.2	1.1 ± 0.1

A number of points can be made here. When it is demanded that the q-values be the same for H I and H_2 the q-value for $E_\gamma > 100$ MeV (1.70 ± 0.04), 10^{-26} cm^{-2} s^{-1} sr^{-1} is seen to be somewhat lower than the canonical value of 2.2×10^{-26}; furthermore, the fit is not too good in the range 300–5000 MeV. However, when the condition of equality of the q-values is relaxed, the situation improves. Perhaps fortuitously the average q-value for the latter situation (the average of q_1 and q_2) is close to 2.2×10^{-26}. The situation where H_2 is more effective at generating γ-rays than H_1 is clearly preferred, although it cannot be regarded yet as a proven fact.

Despite the disclaimer, it is of value to examine possible physical causes of the difference (it is noteworthy that the difference is greatest at the highest γ-ray energies where the angular resolution is best and the significance of the data is greatest). There are several factors which may be invoked, as follows.

(i) Some significant increases in cosmic-ray flux associated with molecular hydrogen will enhance q_2 at the expense of q_1. As remarked earlier, we are not claiming that *all* molecular clouds are inert and pervaded by the ambient cosmic-ray intensity – some do appear to have an enhanced intensity.

(ii) There are undoubtedly *some* discrete sources of γ-rays (such as pulsars) and, insofar as other young objects will be associated with molecular clouds, the γ-sources will be likewise (elsewhere, Issa *et al.* 1981a, we argue that ~ 20 per cent of the γ-flux comes from such sources).

(iii) There is always the possibility that, despite our efforts, the conversion from CO to $N(H_2)$ is incorrect and that H_2 has been underestimated.

At present it is not possible to determine the respective contributions from the factors considered above although the effects referred to in (i) and (ii) are probably dominant.

4.2 RANGE II (l : 100–180°)

4.2.1 Intensity contours

Comparison can be made first between the predicted contours of Fig. 2(d) and the *SAS-2* results (Fig. 2g) and the cut along $b = 0°$ for *COS-B* (Fig. 3). There is seen to be a superficial similarity in that all show a fall-off of γ-ray intensity with increasing longitude; such a trend is expected, of course, whatever galactic origin is suggested for the γ-rays. The predicted peak near 110° is seen to be reflected in the *COS-B* data for both energy regions (Fig. 2e and f) as well as the total (Fig. 3) but the remaining (smaller) predicted peaks are not reproduced; in fact, in view of the limited statistical accuracy of the γ-ray data it is probably unreasonable that they should be. The longitude-dependence is seen to be rather more marked for the observed intensities than for the predicted intensities; this feature is probably due to the fall-off of cosmic-ray intensity with increasing galactocentric radius, R, as claimed by Dodds, Strong & Wolfendale (1975), Issa *et al.* (1981a) and others and will be discussed in more detail later.

4.2.2 Significance of H_2 as a target for cosmic rays

Although there is a distinct correlation of the H_2 peaks with claimed γ-ray sources (see next section) the actual column densities of molecular hydrogen are so low that the contribution to the total column density of gas is negligible and it is not possible to make a useful analysis in the manner indicated previously in Section 4.1.2.

4.2.3 Discrete 'sources'

The region under study contains the two claimed *COS-B* γ-ray sources: 2CG 121 + 04 and 2CG 135 + 01 already referred to. The former is not seen in *SAS-2* but there is support for the latter in the sense that *SAS-2* (Fig. 2g) shows a peak in the same region.

Inspection of Fig. 2(a) shows no corresponding features in atomic hydrogen but Fig. 2(b) and (c) appear to show identification with particular molecular cloud complexes: 2CG 121 + 4 is close to a complex in the 'near' region and 2CG 135 + 01 is almost coincident with a dense 'cloud' in the 'far' region (the latter is the complex CAS OB6). The nearness of the sources to the clouds is so good that we must consider the identifications to be very likely. The extent to which the 'sources' can be explained in terms of CR interactions with the molecular clouds is not clear. Taken at face value enhanced CR intensities within the clouds are necessary (see Issa & Wolfendale 1981, for discussion of 2CG 135 + 01 (CAS OB6) which indicated that enhancement by a factor 10 was necessary) but the small numbers of γ-rays detected and the resulting possibility of fluctuations are a worry.

There are two other effects which need to be considered for 'far' clouds towards the anti-centre: the metallicity gradient and the cosmic-ray gradient. The former affects the conversion from CO $\rightarrow$ H_2 and has been discussed by Blitz & Shu (1980) and ourselves elsewhere (in press); briefly, following the work of Pagel & Edmunds (1981) it seems that the ratio of CO/H_2 should be larger in the inner Galaxy and smaller in the outer Galaxy, typically by a factor 2 at $R = 14$ kpc in comparison with the local value. Thus, the 'far' clouds of Fig. 2(c) have their masses underestimated by about 2; however, this is where the other factor must be considered – the effect of a cosmic-ray gradient (see Section 5) – and this has just the opposite effect, viz. a reduction in cosmic-ray intensity by about 2 at $R \approx 14$ kpc. The net effect is that the enhancement required is hardly changed.

Returning to the 'near' region, 2CG 121 + 04 may indeed be a discrete source but its non-observation by *SAS-2* (Fig. 2g) gives cause for concern.

4.2.4 Derivation of γ-ray emissivities

The procedure adopted in Section 4.1.4 has been followed here, too, viz. the correlation of γ-ray intensity with column density of H I and H_2 has been examined (contributions from discrete sources are ignored, as before). The same relation connecting I_γ with the column densities and q-values has been used.

Table 2 gives the results divided further into two ranges of longitude. The values relate to H I alone; those for H_2 are not useful and are not considered because the very small contribution of molecular hydrogen to the total gas density causes large uncertainties in q_2.

The significance of the values is discussed in the next section.

5 Trend of emissivities with longitude

Fig. 3 shows that the observed intensity (for $E_\gamma > 100$ MeV) along $b = 0^\circ$ falls below expectation for a constant cosmic ray intensity as one proceeds into the outer Galaxy, i.e. $l > 90^\circ$. Insofar as $b = 0^\circ$ corresponds to contributing distances at a maximum distance from the Sun this plot probably represents the best evidence from the present data for a 'cosmic-ray gradient' in the outer Galaxy. It is noted that the effect is not large and indeed its presence depends rather critically on the adopted column density of atomic hydrogen. There is rather more confidence in the gradient, however, than would appear from this plot for a number of reasons.

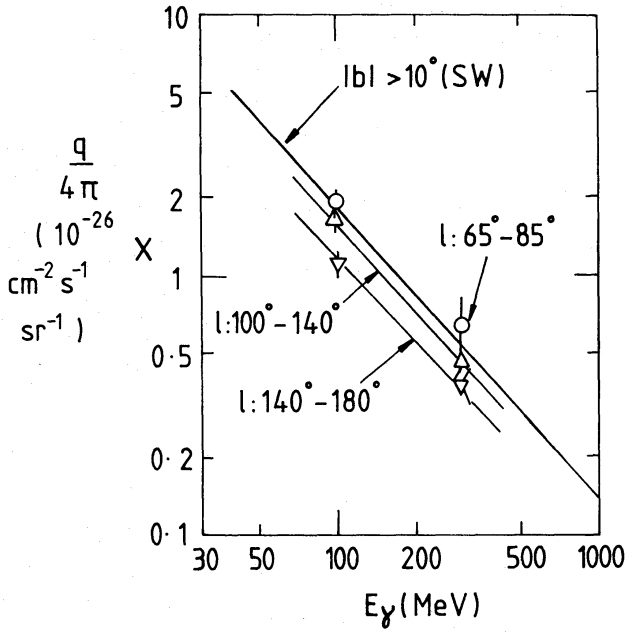

Figure 4. Gamma-ray emissivity $q(>E_\gamma)/4\pi$ versus γ-ray energy for different regions. The line marked SW relates to the local region of the Galaxy in that it comes from analysis of both *COS-B* and *SAS-2* data for $|b|>10°$ (Strong & Wolfendale 1981). The remaining lines are drawn through points derived from the present analysis ($|b|$ less than 4 or 5°). Taken together the data give evidence for a lower q-value and thus lower cosmic-ray intensity, in the outer Galaxy.

(i) The column densities of H I are probably still underestimated somewhat (the effect of cold hydrogen; Davies 1982).

(ii) The metallicity gradient, if continued into the outer Galaxy could well cause the column densities of H_2 to have been seriously underestimated and to contribute about 20 per cent at $l \gtrsim 135°$ instead of being negligible as is the case here.

The actual derived emissivities for various energy ranges are shown in Fig. 4 for the longitude ranges in turn, where they are compared with what would be expected if the cosmic-ray intensity were the same everywhere and equal to the local intensity (the line marked 'SW' – see caption). The emissivities from the present analysis are the averages of the q-values given in Tables 1(b) and 2; the disparity between q_1 and q_2 in Table 1(b) is a worry but the average of q_1 and q_2 is seen to be close to q_{12} (the adopted values are found by averaging q_{12} and the mean of q_1 and q_2). The errors indicated are, inevitably, rather approximate estimates. The small reduction in average emissivity with increasing mean longitude is seen; this result is as would have been expected if the average cosmic-ray intensity were lower in the outer Galaxy.

6 Conclusions

The important rôle of molecular hydrogen in explaining the observed γ-ray intensities has been demonstrated. For longitudes less than 100°, where H_2 is an important ingredient of the ISM, its inclusion enables the bulk of the γ-ray intensity to be understood in terms of the interaction of ambient cosmic rays with the gas in general. That this mechanism alone is not responsible is suggested by the observation that molecular hydrogen is 'more efficient' at generating γ-rays than H I. Coupled with the identification of coincidences between claimed γ-ray 'sources' in the outer Galaxy and the limited concentrations of H_2 gas there is some

evidence present for either discrete sources of γ-rays associated with molecular clouds or, more likely, sources of cosmic rays within clouds which enhance the cosmic-ray intensity there.

The 'cosmic-ray gradient', claimed first from analysis of *SAS-2* data (Dodds *et al.* 1975) and since confirmed, albeit not strongly, by other workers appears still to be acceptable although it is not very marked in the quadrant studied. The reason for its smallness probably lies in the presence of the Perseus arm beyond the solar circle with which both gas and (probably) cosmic-ray sources are associated. The strongest evidence for the gradient appears in the third quadrant (a region not considered in the present work) where low γ-ray intensities appear and where, despite significant amounts of gas, stellar activity is low.

References

Blitz, L. & Shu, F. H., 1980. *Astrophys. J.*, **238**, 148.
Bloemen, J. B. G. M. *et al.*, 1981. *Proc. 17th Int. Cosmic Ray Conf., Paris*, **1**, 181.
Burton, W. B., 1976. *A. Rev. Astr. Astrophys.*, **14**, 275.
Cohen, R. S., Cong, H., Dame, T. M. & Thaddeus, P., 1980. *Astrophys. J.*, **239**, L53.
Davies, R. D., 1982. *Proc. Queen Mary College Conf., Paris*, **1**, 214.
Dodds, D., Strong, A. W. & Wolfendale, A. W., 1975. *Mon. Not. R. astr. Soc.*, **171**, 569.
Dodds, D., Wolfendale, A. W. & Wdowczyk, J., 1976. *Mon. Not. R. astr. Soc.*, **176**, 345.
Fichtel, C. E., *et al.*, 1978. *NASA Tech. Mem. 79656*, G.S.F.C., Greenbelt.
Gordon, M. A. & Burton, W. B., 1976. *Astrophys. J.*, **208**, 346.
Hermsen, W., 1980. *PhD thesis*, University of Leiden.
Hermsen, W., 1981. *Gamma Ray Astronomy*, Royal Society, London, 27.
Issa, M. R., Riley, P. A., Strong, A. W. & Wolfendale, A. W., 1981a. *J. Phys. G*, **7**, 656.
Issa, M. R., Riley, P. A. & Wolfendale, A. W., 1981b. *Proc. 17th Int. Cosmic Ray Conf., Paris*, **1**, 214.
Issa, M. R. & Wolfendale, A. W., 1981. *Nature*, **292**, 430.
Lebrun, F. & Paul, J. A., 1979. *Proc. 16th Int. Cosmic Ray Conf., Kyoto*, **12**, 13.
Li, T. P. & Wolfendale, A. W., 1981a. *J. Phys. G.*, **7**, L157.
Li, T. P. & Wolfendale, A. W., 1981b. *Astr. Astrophys.*, **100**, L26.
Mayer-Hasselwander, H. A., *et al.*, 1980. *9th Texas Symp. Rel. Astrophys., Ann. N.Y. Acad. Sci.*, **336**, 211.
Mayer-Hasselwander, H. A., *et al.*, 1982. *Astr. Astrophys.*, **105**, 164.
Pagel, B. E. J. & Edmunds, M. G., 1981. *A. Rev. Astr. Astrophys.*, **19**, 77.
Protheroe, R. J., Strong, A. W. & Wolfendale, A. W., 1979. *Mon. Not. R. Astr. Soc.*, **188**, 863.
Strong, A. W. & Wolfendale, A. W., 1981. *Phil. Trans. R. Soc. A.*, **301**, 541.
Thaddeus, P., 1981. *Phil. Trans. R. Soc. Lond. A.*, **303**, 469.
Weaver, H. & Williams, D. R. W., 1973. *Astr. Astrophys. Suppl.*, **8**, 1.